

Low Prandtl number convection in layers heated from below

V. KEK and U. MÜLLER

Kernforschungszentrum Karlsruhe GmbH, Institut für Angewandte Thermo- und Fluidodynamik,
Postfach 36 40, W-7500 Karlsruhe 1, Germany

(Received 8 July 1992 and in revised form 27 November 1992)

Abstract—Experimental results are presented for the heat transfer across a horizontal layer of liquid sodium heated from below. The experiments show that up to a Rayleigh number of $Ra \sim 7000$ heat is mainly transferred by conduction for this low Prandtl number fluid. Beyond this threshold value the heat transport by convection increases significantly. For higher values of the Rayleigh number the measured Nusselt numbers follow a power law $Nu \sim Ra^{0.2}$ which is slightly smaller than the one predicted for the so-called flywheel convection as suggested by Jones *et al.* [*J. Fluid Mech.* 73, 353–388 (1976)].

1. INTRODUCTION

THE HEAT transport through plane liquid layers heated from below has received considerable attention, both experimentally and theoretically for moderate and high Prandtl numbers. The existing experimental work is discussed in some detail, by O'Toole and Silveston [1], Rossby [2] and more recently by Threlfall [3] among others. Numerical simulation of the three-dimensional convection and heat transfer problem has been performed only in a limited number of cases and for very few values of the Prandtl number mostly for air with $Pr \sim 0.71$. Such calculations have been published by Lipps [4], Veltishchev and Zelin [5], Grötzbach [6], and McLaughlin and Orszag [7]. The limitations of storage capacity and the computational speed of even very advanced computers still render the accurate prediction of the natural convection in extended layers at high Rayleigh numbers a difficult task. Nevertheless, there are experimental and theoretical data available for a comparative evaluation. The situation is much more unfavourable for the case of very small Prandtl numbers typically for liquid metal flow with $Pr \leq 0.025$ as shown by Meneguzzi *et al.* [8]. Although this kind of flow is of considerable technical importance, precise experimental data for heat transfer are scarce. Thus, even simple and idealized theoretical models published in the literature lack from comparison with experimental findings. The work presented is intended to reduce this deficiency of experimental data for heat transfer and the thermal structure of convection in liquid layers of very low Prandtl number, in our case a liquid sodium layer with $Pr = 0.0058$.

Before we outline in detail the experimental program and procedure we summarize the relevant literature of the problem. Globe and Dropkin [9] performed among other experiments some tests in mercury layers, $Pr = 0.025$, in a Rayleigh number

range $1.5 \times 10^5 < Ra < 4 \times 10^7$. They found that the measured heat transfer data for a mercury layer are represented by the empirical correlation for the Nusselt number Nu in the form

$$Nu = 0.069Ra^{0.33} Pr^{0.074} \quad (1.1)$$

which—according to their findings—also holds for other liquids of higher Prandtl number in the range $0.02 < Pr < 8750$. The evaluated Nusselt numbers for mercury, however, show in the particular plot of experimental data noticeably lower values compared to the data of other liquids.

McDonald and Connolly [10] measured the heat transfer from a hot sodium pool to a downward facing horizontal plate. They derive the empirical relationship

$$Nu = 0.0785Ra^{0.32} \quad (1.2)$$

for the range of Rayleigh numbers $4.8 \times 10^6 < Ra < 4 \times 10^7$. The functional relationship of both formula (1.1) and (1.2) indicates by the $\frac{1}{3}$ -power law that the heat transfer is governed by a fully developed turbulent convection in which external length scales are insignificant (see Howard [11]). However, if in relationship (1.1) the value $Pr = 0.004$ for sodium under the particular test conditions of McDonald and Connolly is inserted the constant of proportionality is smaller by a factor of two compared to that in relationship (1.2).

Kudryavtsev *et al.* [12] conduct heat transfer measurements in sodium using a cylindrical container of aspect ratio height/diameter, $h/D = 1$. For the range $2.5 \times 10^3 < Ra Pr < 8 \times 10^3$ they find the relationship

$$Nu = 0.38(Ra Pr)^{0.33} \quad (1.3)$$

An evaluation of this formula for $Pr = 0.0043$ gives $Nu = 0.062Ra^{0.33}$. Based on empirical and rational arguments Kutateladze [13] proposes for the tur-

heat transport increases significantly when horizontal liquid layers with low Prandtl number are heated from below, and what is the correlation for the heat transfer function?

These questions were considered in several numerical and analytical investigations. Jones *et al.* [16] investigated the convective heat transfer in an axisymmetric cell with stress free boundaries everywhere and with isothermal horizontal but adiabatic vertical boundaries. They found for the limiting case $Pr \rightarrow 0$ a second critical Rayleigh number for the onset of convective heat transfer. Although even below this second critical value there exists free convection in the liquid layer they claim that the convective heat transport is suppressed by a strong nonlinear effect of advection of momentum. Only when this inhibiting nonlinearity of momentum exchange vanishes by a particular alignment of streamlines and vorticity isolines, resembling that of a rigid body rotation, does the intensity of convection increase significantly and as a result the effective heat transfer. The authors call this observation the 'flywheel' effect. It is evident that such an effect may also occur in the case of rigid boundaries, if the local Reynolds number of the velocity distribution becomes high enough to concentrate the viscous dissipation into thin boundary layers near the walls, while in the interior domain rigid body rotation prevails. Recently, Munding [17] has repeated the numerical calculations of Jones *et al.* for rigid boundaries at the top and bottom of the heated layer and for stress free vertical boundaries. He obtained qualitatively similar results. The principal results of Jones *et al.* [16] have been confirmed by Proctor [18] by analytical calculations of two-dimensional natural convection in a horizontal circular cylinder heated at the lower semi-surface and cooled at its upper one. Proctor's investigations were based on non-slip boundary conditions for the velocity and constant surface temperatures. His asymptotic solutions clearly demonstrate the occurrence of a balance between buoyancy and inertial forces for $Pr \rightarrow 0$ and for Rayleigh numbers exceeding a second critical value. He also found that only beyond this second critical value the Nusselt number increases above the level of pure heat conduction. Clever and Busse [19] treated the same problem, namely two-dimensional convection in a horizontal layer, in two articles employing direct numerical simulation by spectral methods and analytical modelling. From their numerical calculations they concluded that for decreasing values of the Prandtl number the onset of a significant heat transport by convection occurs only for increasing supercritical Rayleigh numbers which seem to tend towards a limiting value. A second result of their two-dimensional calculation is that the Nusselt number becomes practically independent of the Prandtl number for Rayleigh numbers $Ra > 10^4$. A comparison between the calculated Nusselt numbers and experimental findings of, for example, Krishnamurti [20] and Rossby [2] shows that there

is a considerable qualitative discrepancy between the predictions of two-dimensional numerical simulations and the experimental data of three-dimensional convection in extended horizontal layers. Only recently published numerical results of Clever and Busse [21], which take into account three-dimensional flow, indicate that three-dimensional effects reduce the value of the predicted Nusselt number considerably and improve the comparison between measured and calculated data for the heat flux and the temperature.

In their analytical investigation Busse and Clever [22] assumed that the bulk velocity field is equivalent to that of a rigid body rotation except in very thin boundary layers near the lower and upper boundary of the layer which they neglect. This model assumption corresponds to the flywheel idea of Jones *et al.* [16]. Using an Oseen approximation in the heat transport equation they obtained the result that for very small Peclet numbers, $Pe = (Ra Pr)^{1/2} \ll 1$, the onset of convective heat transfer occurs only beyond a threshold Rayleigh number Ra_{c2} . For two rigid isothermal boundaries of the layer this value is

$$Ra_{c2} = 7373.$$

They also derived from their model an asymptotic relationship for the Nusselt number for very large Peclet numbers $Pe \gg 1$

$$Nu - 1 \approx \frac{3\pi}{64} (2Ra)^{0.25}. \quad (1.8)$$

This relationship agrees well with the empirical relationship of Rossby [2]. Moreover it supports their numerical findings, namely, the heat transfer becomes independent of the Prandtl number for high values of the Rayleigh number.

This survey of the relevant literature underlines the need for additional experimental investigations of the heat transfer mechanism. The experimental investigations presented in this article are performed in order to validate existing theoretical findings and to reduce existing discrepancies between experiment and theory.

2. EXPERIMENTAL EQUIPMENT AND TECHNIQUES

2.1. Convection apparatus and measuring devices

Two sets of experiments were performed. Screening tests were carried out in a smaller test chamber with simple instrumentation, while the main experiments were carried out in a well-instrumented larger test chamber.

The test apparatus for the heat transfer experiment is depicted schematically in Fig. 1. The circular test chambers were 210 mm in diameter and 25.6 mm in height and 520 mm in diameter and 15 or 46 mm in height. Liquid sodium was used as the test fluid. The mean operational temperature of the sodium during the experiments was in the range 550–570 K. The

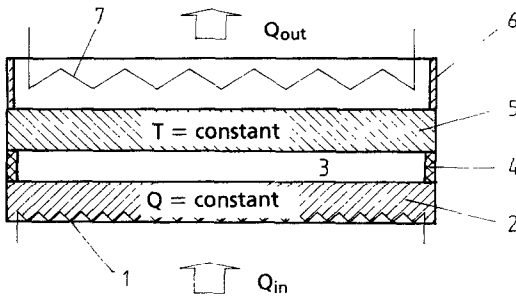


FIG. 1. Schematic drawing of the test apparatus for the main tests, diameter 500 mm, layer height 15.5 mm and 46.5 mm. 1, resistance heater; 2, 5, copper plates; 3, sodium layer; 4, side ring of stainless steel; 6, side wall of boiling cooler; 7, cooling coil.

sodium layer was electrically heated from below by applying a maximum of 17 kW for the smaller, and 40 kW of power for the larger, test chamber through spiral-wound heating conductors brazed to the lower side of a copper plate. For cooling the upper side of the sodium layer another copper plate was used from which the heat was removed either by a sodium cooling circuit or, as done in most of the experiments, by direct evaporative cooling at the upper surface of the cooling plate. Diphyl (Fa. Bayer, Leverkusen) was utilized as a synthetic liquid for evaporative cooling. Circular spacer rings of 15, 25 and 46 mm made of stainless steel formed the side walls of the test chamber. The outside of the entire test apparatus was thermally insulated by a 30 cm thick layer of fiber glass. In order to minimize heat losses from the heating plate in the downward direction additional electrical heating coils were placed in the insulating material at the lower side.

For measuring the temperature at the upper and lower boundaries of the layer boreholes were sunk radially into the copper plates and platinum resistance thermometers were inserted. For the main tests the depth of the boreholes, their position in the plates, and the distance of the borehole tips from the plate surface are listed in Table 1 and shown in Fig. 2. For the screening tests in the small test chamber (diameter 210 mm, height 25.6 mm) the temperature difference was measured by two thermocouples only placed into boreholes of 40 mm in length drilled radially into the upper and lower copper plates.

The experimental program required three different sets of data to be measured, i.e. the heating power,

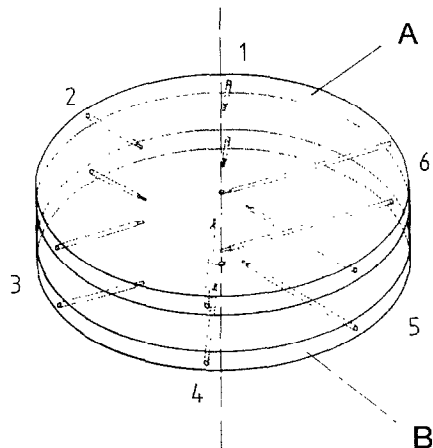


FIG. 2. Arrangement of platinum resistance thermometers Pt-100 in the heater and cooler plate, main tests.

the local temperature differences across the layer at six positions and the temperature on the surface of the insulation at different positions.

The electric power was measured with the aid of four precision resistances of 10 m Ω each to an accuracy of 1%. The surface temperatures of the sodium layer could only be determined indirectly. Resistance probes of the type Pt-100 with a diameter 1.6 mm and with a resolution of $\Delta T = \pm 0.01$ K were inserted into tapered boreholes of 1.8 mm in diameter. Sources of errors in the measurements were local temperature inhomogeneities at the tip of the borehole and thermal contact resistance between the probe and copper wall which could not be precisely determined. Assuming that the probe sensor was positioned with an accuracy of $\Delta h \pm 0.05$ mm and the temperature gradient in the copper plate was 0.05 K mm⁻¹ at an average heat flux of about 2 W cm⁻² the measuring error for the temperature amounts to $\Delta T = \pm 0.0025$ K. The effect of temperature inhomogeneity was neglected because of the high heat conductivity of the copper and the relatively large distance between the outside surface and the tip of the borehole.

The six measuring acquisition systems and peripherals for the temperature probes were calibrated in pretests concerning their linearity and their temperature drift. Moreover, the temperature probes were adjusted to each other by comparison with a reference sensor. The calibration procedure was performed

Table 1. Position of Pt-100 resistance thermometers, main tests

Position	Heating plate		Cooling plate	
1	$r = 80$ mm	$S_{Cu} = 21.15$ mm	$r = 75$ mm	$S_{Cu} = 26.80$ mm
2	$r = 95$ mm	$S_{Cu} = 21.25$ mm	$r = 90$ mm	$S_{Cu} = 26.87$ mm
3	$r = 105$ mm	$S_{Cu} = 21.40$ mm	$r = 100$ mm	$S_{Cu} = 26.98$ mm
4	$r = 155$ mm	$S_{Cu} = 20.95$ mm	$r = 150$ mm	$S_{Cu} = 27.00$ mm
5	$r = 205$ mm	$S_{Cu} = 27.32$ mm	$r = 200$ mm	$S_{Cu} = 27.32$ mm
6	$r = 255$ mm	$S_{Cu} = 20.62$ mm	$r = 250$ mm	$S_{Cu} = 27.57$ mm

under steady-state conditions for a heating power of 1000 W. The calibration was usually repeated after a set of temperature data has been taken. The reproducibility of the calibration data proved to be within the bound of $\Delta T = \pm 0.05$ K.

In order to estimate the heat losses from the test apparatus to the outside, temperatures at various spots at the outer surface of the test chamber and on the surface of the thermal insulation as well as the room temperature were recorded simultaneously.

All the experimental data were recorded and processed by an on-line microprocessor unit combined with an IBM-AT-PC. Details of this unit are described by Kek [23].

2.2. Experimental performance and data evaluation

It was determined that during the experiment special care had to be taken to achieve a quasi-homogeneous temperature distribution in the heating and cooling plates. The measurements showed slight decreasing temperatures in radial direction along the heating plate of the order $\Delta T \approx 1$ K at a heating power of 2000 W and a temperature difference across the layer of about $\Delta T \leq 20$ K. The temperature variation at the cooling plate was even larger without special precautions being taken. In early tests it was determined that the temperature inhomogeneities at the cooling plate could be practically eliminated by removing dissolved oxides from the sodium and by providing a complete wetting between the sodium and the walls of the test chamber. This was achieved by circulating the test fluid for several hours through cold traps in which the oxides were precipitated at cold surfaces outside the test chamber. Moreover, the mean temperature was raised significantly above the operation temperature ($\Delta T \approx +100$ K) in order to achieve a complete wetting between the sodium and the chromium plated copper plates.

To evaluate the heat transfer across the sodium layer accurately the heat losses from the test apparatus to the outside and across the steel rim were determined. This was accomplished by recording the temperature in the copper plates, the surface temperatures of the test apparatus, and the temperature at the surface of the thermal insulation. The heat losses were calculated for the upward, downward, and vertical portions of the cylindrical surface of the insulation. The heat-flow rate through the steel rim was evaluated by direct conduction analysis.

The calculated heat losses were validated for the case of pure heat conduction in the sodium layer at a heating power of 503 W. The calculated heat losses amounted to 196 W in this case compared to the total heat-flow rate through the sodium layer of 306 W. The evaluation of the Nusselt number gave $Nu = 0.94$ and the state of pure heat conduction was predicted to within an error bound of 6%. This result provided the confidence that the heat-flow rate through the layer could be determined by subtracting the evalu-

ated heat losses from the measured total power input to the test apparatus.

In order to present the average heat flux as a function of the driving temperature difference across the sodium layer this temperature difference had to be determined from the measured temperature data. Since the temperature differences across the sodium layer were not directly measured but determined from the temperature measurements in the copper plates the following assumptions were made. It was assumed that by the design of the heating plate a homogeneous heat flux is imposed to the sodium layer. This heat flux is $q = Q/A$, where Q is the total power input and A is the horizontal surface of the sodium layer. If the distance of the top of probe j from the sodium surface is $S_{Cu}^{(H)}(j)$ then the temperature decrease from the probe tip to the layer surface in the heating plate at the location j is

$$\Delta T_H(j) = \frac{Q}{A} \frac{S_{Cu}^{(H)}(j)}{\lambda_{Cu}}, \quad j = 1, \dots, 6, \quad (2.1)$$

where λ_{Cu} is the heat conductivity of the copper. A corresponding expression is obtained for the temperature drop at the location j in the cooling plate. It is

$$\Delta T_{cool}(j) = \frac{Q}{A} \frac{S_{Cu}^{(cool)}(j)}{\lambda_{Cu}}, \quad j = 1, \dots, 6. \quad (2.2)$$

Using these expressions the temperature difference across the sodium layer is

$$\Delta T_{sod}(j) = \Delta T_{tot}(j) - \Delta T_H(j) - \Delta T_{cool}(j), \quad (2.3)$$

where ΔT_{tot} is the measured temperature difference at location j between the thermocouples in the copper plates.

A local heat transfer coefficient $\alpha(j)$ according to Newton's cooling law was defined by using the evaluated local temperature difference across the sodium layer

$$Q = \alpha(j) A \Delta T_{sod}(j). \quad (2.4)$$

The total heat transfer by conduction across the layer is

$$Q_L(j) = \lambda_{sod} A \frac{\Delta T_{sod}(j)}{h}, \quad (2.5)$$

where λ_{sod} is the heat conductivity of the sodium and h the height of the sodium layer. Using equations (2.4) and (2.5) the following expression for a local Nusselt number results:

$$Nu(j) = \frac{Q(j)}{Q_L(j)} = \alpha(j) \cdot \frac{h}{\lambda_{sod}}. \quad (2.6)$$

Because the temperature was not completely uniform across the heating and cooling plates the corresponding inhomogeneous local heat fluxes could not be determined. Therefore an average heat transfer coefficient $\bar{\alpha}$ was introduced and defined as

$$\bar{\alpha} = \frac{1}{n} \sum_{j=1}^n \frac{q(j)}{\Delta T_{\text{sod}}(j)}, \quad j = 1, \dots, 6, \quad (2.7)$$

where for the local heat flux $q(j)$ the average value $\bar{q} = Q/A$ was introduced. Thus the heat transfer coefficient is

$$\bar{\alpha} = \bar{q} \frac{1}{6} \sum_{j=1}^6 \frac{1}{\Delta T_{\text{sod}}(j)}, \quad j = 1, \dots, 6 \quad (2.8)$$

and the average Nusselt number is

$$\overline{Nu} = \frac{\bar{\alpha} h}{\lambda_{\text{sod}}}. \quad (2.9)$$

Furthermore the average Rayleigh number was defined as

$$\overline{Ra} = \frac{g \beta h^3}{\kappa \nu} \overline{\Delta T_{\text{sod}}}, \quad j = 1, \dots, 6, \quad (2.10)$$

where β is the coefficient of thermal expansion, κ the thermal diffusivity, and ν the kinematic viscosity of sodium at its mean temperature. ΔT_{sod} is the arithmetic mean value of the local temperature differences across the layer.† For the sake of simplicity the bars in the notation of the dimensionless groups and of other mean values are dropped in the following.

3. EXPERIMENTAL RESULTS

3.1. Heat transfer measurements

The results of the heat transfer measurements are shown in Fig. 3 according to equations (2.4) and (2.7).

The plots in Fig. 3 contain all the measured data for the experiments with the layer heights 15.5, 25.6 and 46.5 mm. For comparison the dashed lines in the plots represent the calculated heat flow rate by conduction only. It can be seen that in the case of the 15.5 mm layer height the measured heat flow differs only slightly from the value obtained from the pure heat conduction solution. In the case of the 46.5 mm layer height the actual heat flow is significantly larger than that obtained from the pure heat conduction solution for higher temperature differences across the layer, i.e. for $\Delta T \geq 2$ K.

A general representation of the measured data is shown in Fig. 4, where the overall Nusselt number is plotted vs the corresponding overall Rayleigh number. The two dimensionless groups are determined according to the defining equations (2.9) and (2.10) using the mean values of the heat transfer coefficient α and the mean temperature difference ΔT across the layer.

In the low Rayleigh number range $1500 < Ra < 8500$ the value of the Nusselt number is close to unity. The heat transfer is governed in this range by heat conduction. Beyond a threshold value of

† In the screening test with just one thermocouple in the heating and the cooling plate the evaluation of the temperature difference across the sodium layer is straightforward. The averaging process of equation (2.7) is reduced to one term.

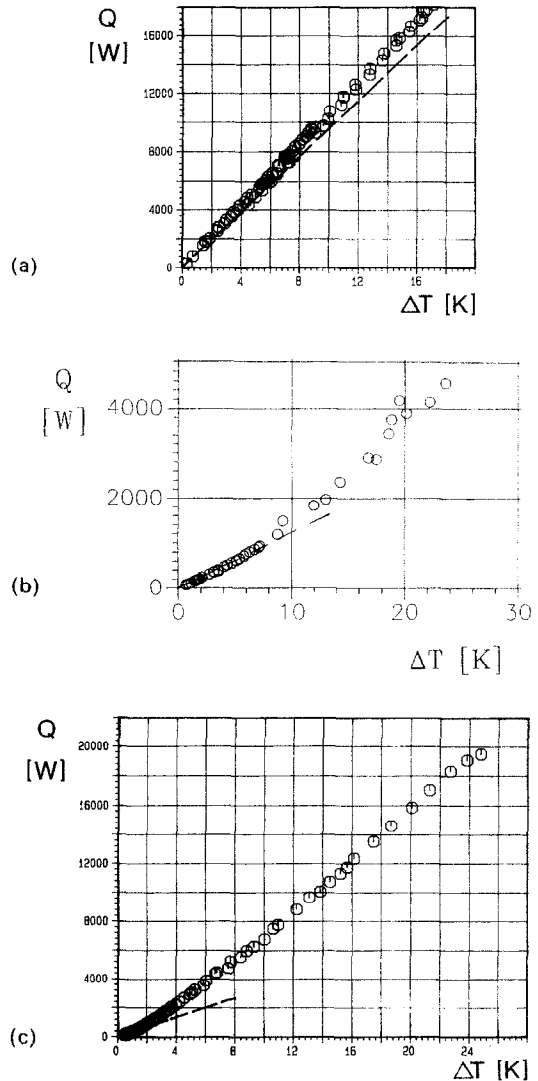


FIG. 3. Mean value of the heat flux as a function of the temperature difference across the sodium layer; (a) layer height $h = 15.5$ cm; (b) layer height $h = 25.6$ mm (screening test); (c) layer height $h = 46.5$ mm; --- calculated conduction heat flux.

$Ra \approx 8000$, a significant increase of the Nusselt number with increasing Rayleigh number is observed which indicates the growing contribution of convective transport to the total heat transfer. The general shape of the data plot in the range $Ra \geq 8000$ can be characterized by a turning point and a negative curvature. Similar properties of the heat transfer function $Nu(Ra)$ for low Prandtl number liquids have been found by Jones *et al.* [16], Busse and Clever [22] and recently by Mundinger [17]. Some of their results are shown in Fig. 7. A more detailed discussion is given in Section 3.2.

For engineering applications it is useful to represent the data sequence in Fig. 4 by correlations in terms of fractional powers of the Rayleigh number. Such correlations are obtained by least-square fit interpolation of the data points. The numerical results of

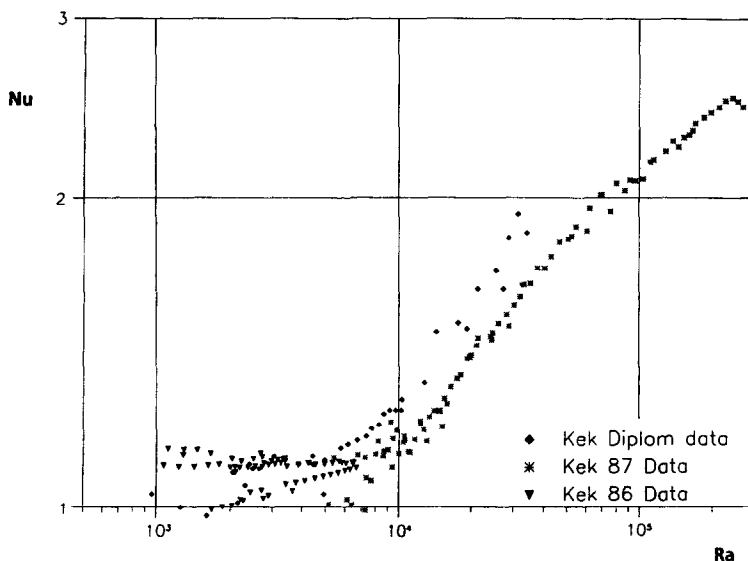


FIG. 4. Nusselt number as a function of the Rayleigh number, Prandtl number $Pr = 0.0058$, ∇ layer height 15.5 mm, layer height 25.6 mm (screening tests), layer height 46.5 mm.

Jones *et al.* [16], Clever and Busse [19] and Munding *et al.* [17] as shown in Fig. 7 suggest three different Rayleigh number ranges for an interpolation of the experimental data, namely a range of prevailing conduction heat transfer, a transition range of strongly increasing convective heat transport starting near the turning point in the Nusselt-Rayleigh number curve and an asymptotic range. The bounds of these ranges are not sharply defined. The following data ranges have been chosen: $1600 < Ra < 7000$, $10^4 < Ra < 5 \times 10^4$, $4 \times 10^4 < Ra < 24 \times 10^4$. The results of the fitting procedure are shown in Fig. 5. Only data of the main tests were used. There is first the range $1600 < Ra < 7000$ of prevailing heat transfer by conduction

$$Nu = 0.59Ra^{0.072}, \quad 1600 < Ra < 7000. \quad (3.1)$$

This correlation was derived from a data sequence obtained in an experiment with particularly uniform temperature distribution on the heating and cooling plates. More details of this experiment are given below. This correlation demonstrates that the convective heat transfer at the relatively high supercritical Rayleigh number $Ra \approx 7000$ is less than 10% of the total heat transfer, a surprisingly low value.

A transition range follows, where heat transfer by convection is promoted according to Jones *et al.* [16] by inertial forces. We define this transition range as $10^4 < Ra < 5 \times 10^4$, and we get

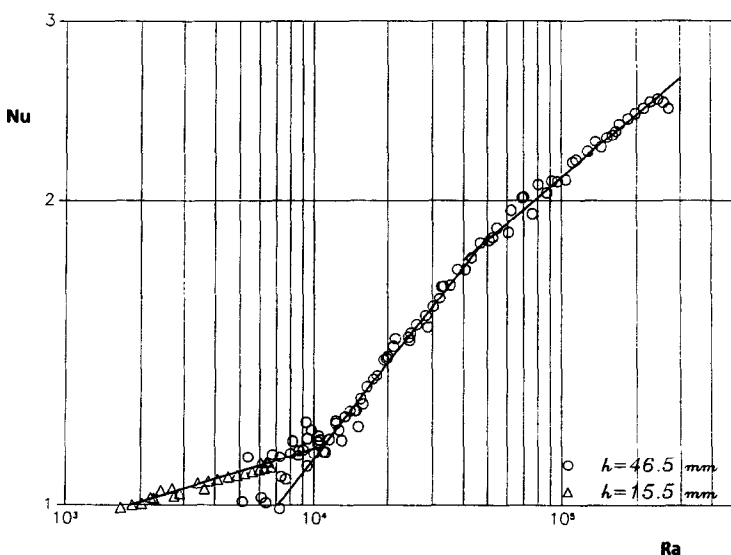


FIG. 5. Fitting curves to the data sequences of the main tests.

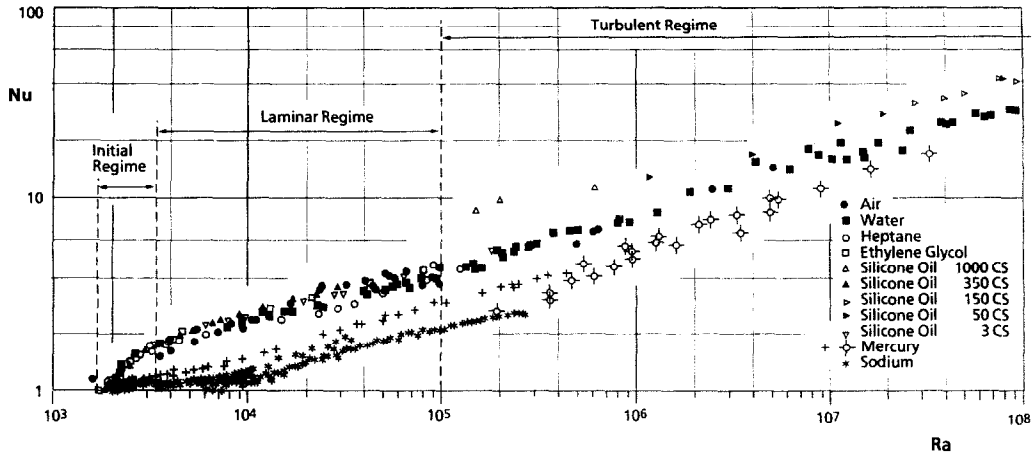


Fig. 6. Experimental data for the Nusselt number vs Rayleigh number relationship. \circ \bullet \blacksquare \triangle \diamond \triangleright \blacktriangledown data compiled by O'Toole and Silverston [1], $+$ data from measurements of Rossby [2], $*$ data from this work.

$$Nu = 0.0616Ra^{0.31}, \quad 10^4 < Ra < 5 \times 10^4. \quad (3.2)$$

For the remaining range of Rayleigh numbers the exponential fit results in the correlation

$$Nu = 0.20Ra^{0.20}, \quad 4 \times 10^4 < Ra < 2.5 \times 10^5. \quad (3.3)$$

It is noted here that the effectiveness of the heat transfer by convection reduces beyond a transition range as the power of the Rayleigh number reduces from 0.31 to 0.20. A similar procedure of piecewise fitting the experimental heat transfer data has been adopted by other researchers in the past, for example, see O'Toole and Silverston [1].

In order to determine the threshold values of the Rayleigh numbers for onset of convection and onset of significant heat transfer by convection the fitted curves are extrapolated to $Nu = 1$. The critical Rayleigh numbers are then defined by the inter-

section points of the fitted curves I and II and the abscissa $Nu = 1$ in Fig. 6. The result is

$$Ra_{c1} = 1819, \quad Ra_{c2} = 7125. \quad (3.4)$$

It is noted here that in order to obtain the fitted curve in the low Rayleigh number range $1600 < Ra < 7000$ a set of 23 experimental data points of one particular experimental run has been chosen. In this run special care was taken to provide a temperature distribution across the heating and cooling plates as uniform as possible. This was achieved by a special cleaning procedure for the liquid sodium in the test chamber to remove uncontrolled thin oxide layers from the surface of the cooling plates which lasted several days. The data sets of other earlier experimental runs suffer from experimental errors of the order of 10% due to local temperature inhomogeneities which did not allow a proper evaluation of a critical Rayleigh number for onset of convection. The critical Rayleigh number for onset of convection obtained from equation (3.1) is about 6% higher than the value $Ra_c = 1708$ according to the theory for perfectly conducting horizontal boundaries. A better result for Ra_{c1} is obtained, when the evaluated data for the Nusselt and Rayleigh number are subjected to a quadratic least-square fit. In this case $Ra_{c1} = 1717$ is obtained.

3.2. Discussion of the results

The striking result of the heat transfer measurements is the peculiar shape of the Nusselt-Rayleigh number function in the range of investigation. A slow increase of the Nusselt number in the range $1.6 \times 10^3 < Ra < 8 \times 10^3$ is followed by a significant growth rate for the Rayleigh numbers $8 \times 10^3 < Ra < 2.5 \times 10^5$. This effect is obviously related only to very low values of the Prandtl number as can be seen from Fig. 6. This figure shows exper-

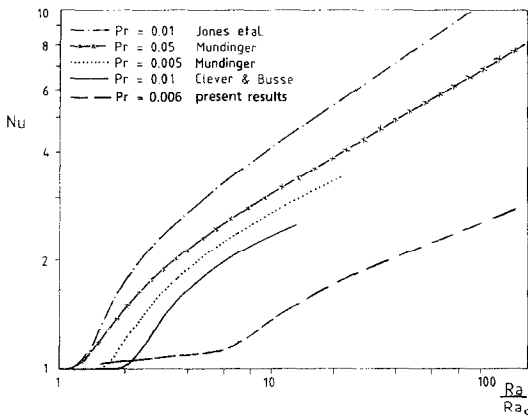


Fig. 7. Calculated Nusselt numbers as a function of the reduced Rayleigh number $r = Ra/Ra_{c1}$, two-dimensional numerical calculations. --- $Pr = 0.01$, Jones *et al.* [16]; — $Pr = 0.05$; ··· $Pr = 0.005$, Mundinger [17], - · - $Pr = 0.01$, Clever and Busse [19].

imental data of various authors compiled by O'Toole and Silveston [1], data of Rossby [2] and data from this work. The functional dependence of the Nusselt-Rayleigh number graph for sodium with $Pr = 0.0058$ is in qualitative agreement with the shape of the calculated curves of Jones *et al.* [16], Clever and Busse [19] and Munding [17]. The calculated curves are shown in Fig. 7. The curves show a delayed increase of the Nusselt numbers in the low range of supercritical Rayleigh numbers. Furthermore, the calculated curves contain a turning point and beyond which a negative curvature. These properties are also present in the data sequence of the present experiments as shown in Fig. 4. There are, however, considerable quantitative discrepancies between the calculated and measured data. The calculations significantly underpredict the second critical Rayleigh number for onset of convective heat transfer and considerably overpredict the amount of convected heat. It is conjectured that these discrepancies originate from very restrictive assumptions made for the calculations, namely, the existence of two-dimensional steady roll patterns only. In the present experiments three-dimensional cellular patterns are certainly present because of the large dimension of the layers and, moreover, the convection is always in a fluctuating mode, i.e. time dependent. It has been known since the investigations of Malkus and Veronis [24] that two-dimensional convection patterns are more efficient in heat transport than three-dimensional patterns. More recent investigations of Clever and Busse [21] on three-dimensional, time-dependent convection strongly support this conclusion. The present experimental results differ also quantitatively from the experimental findings of Chiffaudel *et al.* [14]. In their small box test cell with mercury as the test liquid ($Pr \sim 0.025$) they arranged a two-dimensional convection pattern by choosing an appropriate aspect ratio. They confirm by their heat transfer measurements semiquantitatively the calculated Nusselt numbers of Jones *et al.* [16] and Proctor [18] in a Rayleigh number range $10^3 < Ra < 2.5 \times 10^3$. They also define a second critical Rayleigh number Ra_c by the same procedure as in this work. They find $Ra_{c2} = 1.06Ra_c$. This value is of the order of the calculated values for $Pr = 0.025$ presented in Fig. 7. A detailed comparison with the present results suggests once more a significant influence of the three-dimensional effects in this investigation.

Jones *et al.* [16] and Proctor [18] concluded from their calculations that for the limiting case $Pr \rightarrow 0$ a second critical Rayleigh number exists for the onset of significant convective heat transport. Busse and Clever [22] predicted this value analytically as $Ra_{c2} = 7373$. The threshold Rayleigh number $Ra_{c2} \approx 7125$ obtained from the present experiments is surprisingly close to the value of Busse and Clever [22]. However, it differs significantly from corresponding values suggested by the numerically determined curves in Fig. 7. More theoretical work into

three-dimensional effects is needed to clarify this quantitative discrepancy. Nevertheless, since all the authors base their analysis for the limiting case $Pr = 0$ on the balance between the inertia and the buoyancy force in the momentum equations we conjecture that the experimentally determined shape of our $Nu(Ra)$ curve as well as the so-defined second critical Rayleigh number is to be explained by the same physical effect.

The model calculations for the heat transfer of Busse and Clever [22] based on the 'flywheel' assumption are to some extent supported by the present measurements in the high Rayleigh number range. If one assumes a rigid body rotation for the vortex flow in the convection cell these authors obtain for high values of the product $Ra \cdot Pr$ the following relation for the heat transfer

$$Nu - 1 \approx \frac{3\pi}{64} (2Ra)^{0.25} = 0.175 \times Ra^{0.25}. \quad (3.5)$$

This relationship has to be compared with our correlation $Nu = 0.201 Ra^{0.20}$ for Rayleigh numbers $Ra > 4 \times 10^4$. In spite of the various assumptions and approximations used the two results clearly indicate a significantly reduced convective heat transport compared to the one in liquids of Prandtl numbers of the order one and higher.

A plausible explanation for a power relationship for the heat transfer in low Prandtl number liquids was given by Jones *et al.* [16] using similitude theory. For high Rayleigh numbers the vortex flow in the convection cell develops boundary layers along the walls. For very low Prandtl numbers the thickness of the thermal boundary layer is significantly larger than the boundary layer of the flow field. Actually, the ratio of the boundary layer thicknesses should scale like $\delta_s/\delta_T \sim Pr^{1/2}$, where δ_s and δ_T refer to the flow and temperature field thicknesses, respectively. Jones *et al.* argue that the heat transferred from the wall into the thermal boundary layer by conduction is completely convected from that boundary layer by the rigid body rotation of the bulk flow in the cell center. The characteristic velocity of the rigid body rotation is the buoyant velocity defined by external parameters $U_o = (\beta g \Delta T h)^{1/2}$. The energy balance for the thermal boundary layer of a cell then gives:

$$\lambda \frac{\Delta T}{2} \frac{1}{\delta_T} h^2 \approx U_o \rho c \frac{\Delta T}{2} h \cdot \delta_T \quad (3.6)$$

where λ is the heat conductivity of the liquid, ρ its density and c its capacity. By rearranging the expression and by using the relation $Nu \sim h/\delta_T$ they obtain

$$Nu \sim (Ra \cdot Pr)^{1/4}. \quad (3.7)$$

This power relation is compatible with the empirical correlation of this work and agrees well with the model relationship of Busse and Clever [22]. The arguments together with the experimental results support

the idea that viscous forces concentrated in the boundary layers are irrelevant for the overall heat transfer mechanism in this range of Rayleigh numbers and in the case of very small Prandtl numbers.

Rosby [2] derived from his experiments with mercury layers an empirical relationship showing the functional dependence $Nu \sim Ra^{0.257}$ (see Section 1, equation (1.5)). However, the range of applicability for his correlation extends to very low Rayleigh numbers. In particular, he does not find a distinct change in the slope of the Nusselt–Rayleigh number curve in the range $Ra < 2 \times 10^4$.

Furthermore the present results do not indicate any improvement in heat transfer for Rayleigh numbers $Ra \geq 10^5$. Such an improvement was suggested by some researchers, for example, Globe and Dropkin [9], McDonald and Connolly [10], Kudryavtsev *et al.* [12] in the form of an empirical correlation $Na \sim Ra^{1/3}$. This functional dependence was also obtained from dimensional considerations taking into account boundary layer aspects and some simple ideas of turbulent flow such as mixing length scales and the law of the wall relation for the velocity and temperature distribution. Based on such considerations Kraichnan [25] and Long [26] derive for sufficiently high Rayleigh numbers and small Prandtl numbers the relation $Nu = K(Ra Pr)^{1/3}$, where the coefficient K may depend on the turbulent kinematic viscosity. This relationship holds only when the thickness of the turbulent boundary layer of the velocity is much smaller than the thickness of the heat conduction layer but larger than a comparative viscous sub-layer. Kraichnan derives the following limits for the validity of the $\frac{1}{3}$ -power law for the heat transfer: $(Ra Pr)^{1/3} \geq 6$ and $Ra \geq 9500$. He concludes furthermore that for $(Ra Pr)^{1/2} \leq 6$ the Nusselt number should be $Nu \approx 1$. These results are not compatible with our experimental findings, and the theoretical results of Jones *et al.*, Proctor, and Busse and Clever. The conclusion seems reasonable that the $\frac{1}{3}$ -power law becomes valid only in low Prandtl number fluids for much higher values of the Rayleigh number. Measurements for characterizing the internal structure of the flow are required and, moreover, heat transfer measurements in sodium layers have to be performed up to even higher Rayleigh numbers of the order $Ra \sim 10^{10}$ to resolve this uncertainty.

The authors feel that there is little chance to establish experimental conditions for Rayleigh numbers of the order $Ra \sim 10^{15}$ – 10^{20} , which are typical for the Ledoux [27] and Spiegel [28] correlation $Nu \sim Ra^{1/2}$ derived for astrophysical conditions in gases of extremely low Prandtl number.

REFERENCES

- J. L. O'Toole and P. L. Silveston, Correlations of convective heat transfer in confined horizontal layers. *Chem. Engng Prog. Symp. Series* **67**, 81–86 (1961).
- H. T. Rosby, A study of Benard convection with and without rotation. *J. Fluid Mech.* **36**, 309–335 (1969).
- D. C. Threlfall, Free convection in low-temperature gaseous helium. *J. Fluid Mech.* **67**, 17–28 (1975).
- F. B. Lipps, Numerical simulation of three-dimensional Benard convection in air. *J. Fluid Mech.* **75**, 113–148 (1976).
- N. F. Veltishchev and A. A. Zelin, Numerical simulation of cellular convection in air. *J. Fluid Mech.* **68**, 352–368 (1975).
- G. Grötzbach, Direct numerical simulation of laminar and turbulent Benard convection. *J. Fluid Mech.* **119**, 27–53 (1982).
- J. B. McLaughlin and S. G. Orszag, Transition from periodic to chaotic thermal convection. *J. Fluid Mech.* **122**, 123–142 (1982).
- M. Meneguzzi, C. Sulem, P. L. Sulem and O. Thual, Three-dimensional numerical simulation of convection in low-Prandtl-number fluids. *J. Fluid Mech.* **187**, 169–191 (1987).
- S. Globe and D. Dropkin, Natural-convection heat transfer in liquids confined by two horizontal plates and heated from below. *J. Heat Transfer* **February**, 24–28 (1959).
- J. McDonald and T. J. Connolly, Investigations of natural convection heat transfer in liquid sodium. *J. Nucl. Sci. Engng* **8**, 369–377 (1960).
- L. N. Howard, *Proceedings of the 11th Congress of Applied Mechanics* (Edited by H. Görtler), p. 1109. Springer, Berlin (1964).
- A. P. Kudryavtsev, D. M. Ovechkin, D. N. Sorokin, V. I. Subbotin and A. A. Tsyganok, 'Zhidkie Metally' a collection of papers of liquid metal technology. *Atomizdat* **1967**, 131–136 (1967).
- S. S. Kutateladze *et al.*, *Liquid-Metal Coolants*. Atomizdat, Moskau (1958).
- A. Chiffaudel, S. Fauve and B. Perrin, Viscous and inertial convection at low Prandtl number: experimental study. *Europhys. Lett.* **4(5)**, 555–560 (1987).
- A. Schlüter, D. Lortz and F. H. Busse, On the stability of steady finite amplitude convection. *J. Fluid Mech.* **23**, 129–144 (1965).
- C. A. Jones, D. R. Moore and N. O. Weiss, Axisymmetric convection in a cylinder. *J. Fluid Mech.* **73**, 353–388 (1976).
- G. Mündinger, Numerische Simulation einer Konvektionsströmung in einer Zylindergeometrie. Diplomarbeit Universität Karlsruhe (1989).
- M. R. E. Proctor, Inertial convection at low Prandtl number. *J. Fluid Mech.* **82**, 97–114 (1977).
- R. M. Clever and F. H. Busse, Low Prandtl number convection in a layer heated from below. *J. Fluid Mech.* **102**, 61–74 (1981).
- R. Krishnamurti, Some further studies on the transition to turbulent convection. *J. Fluid Mech.* **60**, 285–303 (1973).
- R. M. Clever and F. H. Busse, Nonlinear oscillatory convection. *J. Fluid Mech.* **176**, 403–417 (1987).
- F. H. Busse and R. M. Clever, An asymptotic model of two-dimensional convection in the limit of low Prandtl number. *J. Fluid Mech.* **102**, 75–83 (1981).
- V. Kek, Benard-Konvektion in flüssigen Natriumschichten, Dissertation Universität Karlsruhe (1989).
- V. W. R. Malkus and G. Veronis, Finite amplitude convection. *J. Fluid Mech.* **23**, 225–260 (1958).
- R. H. Kraichnan, Turbulent thermal convection at arbitrary Prandtl number. *Phys. Fluids* **5**, 1374–1389 (1962).
- R. R. Long, Relation between Nusselt number and Rayleigh number in turbulent thermal convection. *J. Fluid Mech.* **105**, 445–451 (1976).
- P. Ledoux, M. Schwarzschild and E. Spiegel, On the spectrum of turbulent convection. *J. Astrophys.* **133**, 184 (1961).
- E. A. Spiegel, Convection in stars. *Ann. Rev. Astron. Astrophys.* **9**, 323 (1971).